5594 *Chem. Mater.* **2009,** *21,* 5594–5600
DOI:10.1021/cm901708v

CHEMISTRY OF MATERIALS
Article

Gold-Coated Cementite Nanoparticles: An Oxidation-Resistant Alternative to α-Iron

Michael D. Shultz,*,† Scott Calvin,‡ Fernando Gonzalez-Jimenez,§ Vladimiro Mujica,⊥ Blaine C. Alleluia,‡ and Everett E. Carpenter*,†

†*Department of Chemistry, Virginia Commonwealth University, Richmond, Virginia,* ‡*Sarah Lawrence College, Bronxville, New York,* §*Laboratorio de Magnetismo, Escuela de Fisica, Ciencias, UCV, Caracas, Venezuela, and* ⊥*Department of Chemistry, Northwestern University, 2145 Sheridan Road, Evanston, Illinois*

Received June 19, 2009. Revised Manuscript Received September 9, 2009

Iron-based nanoparticles are desirable for many applications because of their magnetic properties and inherent biocompatibility. Metallic iron, or α-Fe, is the most sought after because of its high saturation magnetization (up to 220 emu/g). This magnetization in iron nanoparticles is difficult to reach or maintain because of the ease of oxidation, which greatly reduces the magnetization values (90 emu/g or less). Here, we report the synthesis of an iron-based nanoparticle comprising a magnetic cementite core (Fe_3C) that is more oxidation-resistant than α-Fe, an oxide layer, and a gold coating for passivation and easy functionalization. The nanoparticle structure was confirmed via X-ray absorption fine structure and Mössbauer experiments, and morphology was confirmed using transmission electron microscopy. Magnetic characterization yielded a saturation magnetization of 110 emu/g, thus demonstrating cementite as more stable alternative to α-Fe with higher magnetic moments than the iron oxides.

1. Introduction

Iron-based nanoparticles are a front runner in a vast number of applications because of several key features. First, iron metal has the highest magnetic moment per gram for any material comprising one element. This then leads other materials based on iron, such as ferrites and alloys, to possess numerous variations of magnetic properties, thereby making iron-based nanoparticles extremely versatile and broad reaching in application. Another feature that makes iron-based nanoparticles useful in biomedical applications is iron's innate biocompatibility, which makes integration into biological systems very promising. The major obstacle, however, to the practical use of zerovalent iron-based nanoparticles is the ease of oxidation, resulting in loss of the original magnetic state. Therefore, the synthesis of oxidation resistant iron based nanoparticles with high magnetic moments is of great interest, and vital to achieving the reproducibility required for long-term biomedical studies. One form of iron that potentially can fulfill these requirements is cementite, Fe_3C. This structure is a primary component in carbon steel and is very resistant to corrosion and oxidation. The structure of cementite is a solid solution of zerovalent iron with carbon where the iron atoms in a state similar to a high volume FCC state. (Theoretical calculations indicate that face centered cubic (FCC) iron has four magnetic states. The complexity of the magnetic properties for the FCC iron is primarily linked to different spin states available in the FCC structure that also correspond to slight differences in atomic distances.[1−3]) Magnetic properties of cementite are similar to one of the low-spin ferromagnetic FCC states with a bulk saturation magnetization of 130 emu/g.[4] The carbons distribute to form two different atom environments for the iron, thus altering the individual magnetic moments of the iron. This feature is the primary information that can be used to distinguish the cementite structure from other zerovalent iron structures through techniques that are sensitive to local magnetic environments, such as Mössbauer spectroscopy.

Cementite (Fe_3C) has been reported on the nanoscale, but mainly synthesized via laser pyrolysis and other high-temperature methods.[5,6] As will be shown below, we have synthesized nanoparticles with a cementite core, which yields their dominant ferromagnetic behavior. These nanoparticles also exhibit a much weaker superparamagnetic response associated with antiferromagnetic coupling in an oxide shell surrounding the cementite, which is strongly dependent on temperature because of the existence of fluctuations of the relative orientation of

*Corresponding author. E-mail: shultzmd@vcu.edu (M.D.S.); ecarpenter2@vcu.edu (E.E.C.).

(1) Krasko, G. L. *Phys. Rev. B* **1987**, *36*, 8565–8569.
(2) Moruzzi, V. L.; Marcus, P. M.; Schwarz, K.; Mohn, P. *Phys. Rev. B* **1986**, *34*, 1784–1791.
(3) Wang, C. S.; Klein, B. M.; Krakauer, H. *Phys. Rev. Lett.* **1985**, *54*, 1852–1855.
(4) David, B.; Schneeweiss, O.; Mashlan, M.; Santava, E.; Morjan, I. *J. Magn. Magn. Mater.* **2007**, *316*, 422–425.
(5) Alexandrescu, R.; Morjan, I.; Dumitrache, F.; Birjega, R.; Jaeger, C.; Mutschke, H.; Soare, I.; Gavrila-Florescu, L.; Ciupina, V. *Mater. Sci. Eng., C* **2007**, *27*, 1181–1184.
(6) Narkiewicz, U.; Pelech, I.; Roslaniec, Z.; Kwiatkowska, M.; Arabczyk, W. *Nanotechnology* **2007**, *18*, 405601.

 Published on Web 11/04/2009

the surface moments with respect to their own anisotropy axis. This complex magnetic behavior and the fact that the two components can be decoupled at low temperatures is one of the most interesting findings of this study.

This work thus describes the synthesis and characterization of cementite-based nanoclusters that are air stable at room temperature and ambient pressure. The stability is due to partially the inherent corrosion resistance of cementite itself and partially to the use of a gold-based oxidizing agent to create a very thin iron oxide and gold layer around the small cementite cores. This layer not only aids in the prevention of further oxidation but also allows for easier functionalization. A third reason that the gold layer was chosen was that theoretical work has shown the possibility for gold monolayers to enhance magnetic properties through spin−orbit coupling.[7]

2. Experimental Section

2.1. Synthetic Methods. Fe_3C nanoparticles were synthesized via a high temperature spontaneous nucleation technique involving the decomposition of iron pentacarbonyl ($Fe(CO)_5$) in the presence of refluxing trioctylphosphine oxide (TOPO).[8,9] The particles in TOPO were then placed in the presence of Au^{3+} as per the following example. In a typical synthesis, 5 g of TOPO was heated to reflux with an air condenser under a nitrogen atmosphere. Then, 0.20 mL of $Fe(CO)_5$ was injected in the hot TOPO and allowed to age for 30 min. During the 30 min, a mixture of 30 mL of diphenyl ether and 0.20 g of $Au(O_2CCH_3)_3$ was heated to 100 °C while vigorously stirring. At the 28 min mark, 4 mL of 200 MW PEG was added to the Au/ether mixture as a mild reducing agent. Then at the end of the initial 30 min, the Fe/TOPO solution was transferred into the Au/PEG/ether solution and allowed to age for another 30 min. At this point, the solution appeared black/purple in color. The reaction was quenched by bringing the mixture quickly to room temperature by pouring the solution into 200 mL of methanol. The nanoparticles were then treated with subsequent washing in acetone and methanol and magnetically extracted to dry.

Uncoated nanoparticles were also prepared to aid in obtaining structural information and insight into the mechanism by which the Au was coating the surface. The uncoated samples were prepared in similar fashion to the coated samples by injection of $Fe(CO)_5$ into refluxing TOPO. In the uncoated case however, after the initial 30 min in TOPO, the reaction was quenched in acetone and subsequently washed further with acetone and methanol, followed by magnetic extraction and drying. As the uncoated samples were not air stable, they were maintained in a nitrogen atmosphere before and during characterization.

2.2. Characterization Methods. To identify the different phases of iron, we used Mössbauer Spectroscopy (MS) on the 14.4 keV transition of ^{57}Fe. The source is ^{57}Co in Rh and the spectrometer is a homemade combination of a driver, multichannel scaling system (MCS), and nuclear detection chain with a proportional counter, which was run in the triangular symmetric mode. The instrument was calibrated with α-Fe and the isomer shifts are given relative to it. The spectra were computer-fitted with Lorentzian shapes for the lines and a limited number of free parameters (3) for each subspectrum. The temperature of the samples was varied by placing them on a cryostat, which allowed work in a temperature range from room to liquid helium conditions.

To ensure the samples remain unoxidized during shipping, they were shipped for Mossbauer under mineral oil that was degassed with nitrogen and packaged in the glovebox. They were analyzed promptly upon arrival and then again several more times during 6 months. Each spectrum was similar, and only the last one is presented in this paper.

For confirmation, XAS spectroscopy was employed. Iron K edge and gold L-III edge transmission X-ray absorption spectra (XAS) were collected at beamline X-11B at the National Synchrotron Light Source, and analyzed using the Ifeffit and Horae packages.[10,11] The samples were prepared by grinding the powder with a mortar and pestle and then spreading thin layers of the finely ground powder on multiple layers of Kapton tape. The number of layers of tape was chosen so as to make the iron absorption edge jumps between 0.1 and 1.0. The channel-cut monochromator was detuned approximately 40% before measuring each edge. At least two scans were averaged for each edge of each sample. For each edge, the corresponding metal foil was measured in a reference channel.

As with Mossbauer additional precautions were taken to ensure the sample integrity. Several different techniques were used, including preparing the XAS samples in the glovebox, heat sealing them in polyethylene bags, and shipping them in seal glass vials. The samples were analyzed on two different beamlines over 4 months after the initial studies. As with the Mossbauer, the data during the multiple runs were consistent and only the last spectra were used because of space constraints.

3. Results and Discussion

3.1. Imaging. The diameter of the resulting particles is 2−4 nm as seen by transmission electron microscopy. The TEM image obtained is shown in Figure 1 with a histogram showing a mean diameter of 2.73 nm inset in the figure. Scanning tunneling electron microscopy−energy-dispersive spectrometry analysis (available in the Supporting Information) revealed changes in both the Fe and Au concentrations while scanning across the nanoparticles, thus suggesting some amount of Au being present on the surface of the Fe_3C cores.

3.2. XAFS Structural Analysis. Figure 2 shows the X-ray absorption near edge (XANES) spectra for the coated and uncoated samples, a metal foil, and an oxide standard. For comparison, a linear combination made up of equal parts of the two standards is also shown. Best-fit linear combinations of the two standards suggest 40−50% zerovalent iron for the coated sample, and 65−75% zerovalent iron in the uncoated sample. The XANES results should be treated as only semiquantitative, since both the zerovalent and oxidized phase in the nanoparticle are likely to differ somewhat from the standards used. Nevertheless, it is clear that the uncoated sample is less oxidized than the coated sample.

(7) Sun, Q.; Kandalam, A. K.; Wang, Q.; Jena, P.; Kawazoe, Y.; Marquez, M. *Phys. Rev. B* **2006**, *73*, 134409.
(8) Murray, C. B.; Norris, D. J.; Bawendi, M. G. *J. Am. Chem. Soc.* **1993**, *115*, 8706–8715.
(9) Park, S. J.; Kim, S.; Lee, S.; Khim, Z. G.; Char, K.; Hyeon, T. *J. Am. Chem. Soc.* **2000**, *122*, 8581–8582.
(10) Newville, M. *J. Synchrotron Radiat.* **2001**, *8*, 322–324.
(11) Ravel, B.; Newville, M. *J. Synchrotron Radiat.* **2005**, *12*, 537–541.

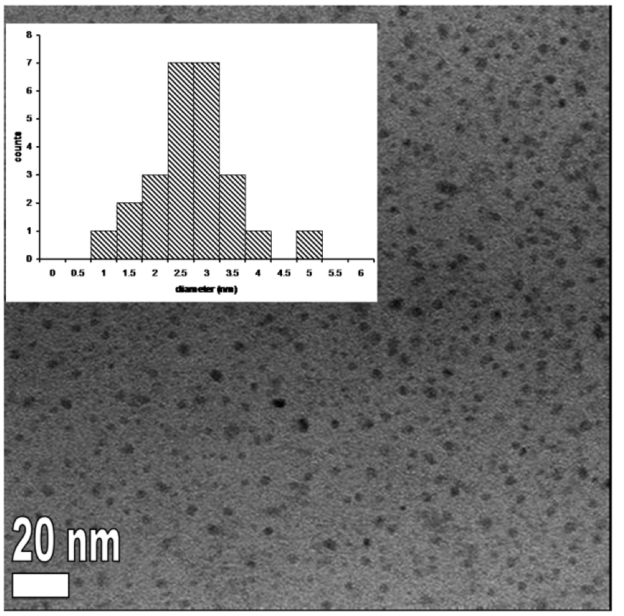

Figure 1. TEM image of the nanoparticles as prepared on a Cu mesh grid. The TOPO cap was washed by and substituted with pyridine prior to grid preparation. The inset is a histogram of line measurements performed across the nanoparticles on the image.

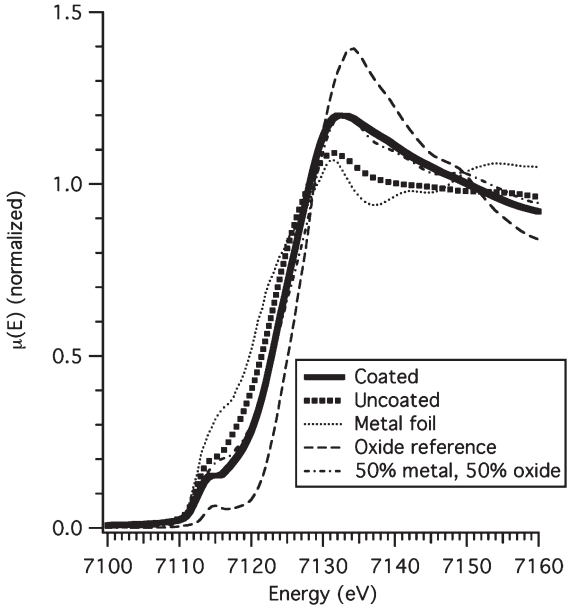

Figure 2. XANES at the iron K edge of samples and standards. A linear combination consisting of equal contributions from the foil and oxide is also shown for comparison.

The extended X-ray absorption fine structure (EXAFS) spectra were analyzed by fitting the spectra to ab initio theoretical standards.[12] Background subtraction was performed using the method of Newville et al.,[13] with a cutoff frequency for the background spline of 1.0 Å. After background subtraction, data were transformed to a function of photoelectron wavenumber k. Because EXAFS amplitude generally falls off with increasing k, the data were multiplied by k^2 prior to taking the Fourier transform

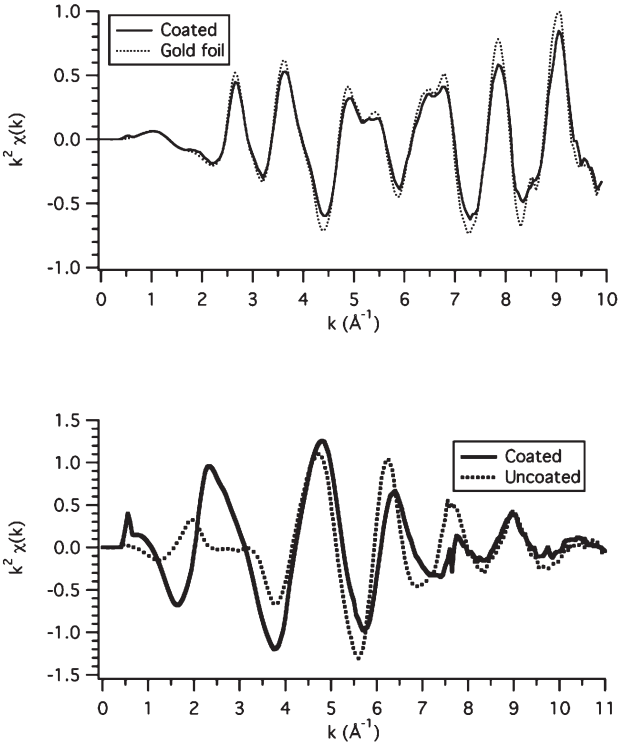

Figure 3. (top) EXAFS spectrum for gold L III edge of coated sample, with gold foil for comparison. (bottom) EXAFS spectrum for iron K edge of coated and uncoated samples.

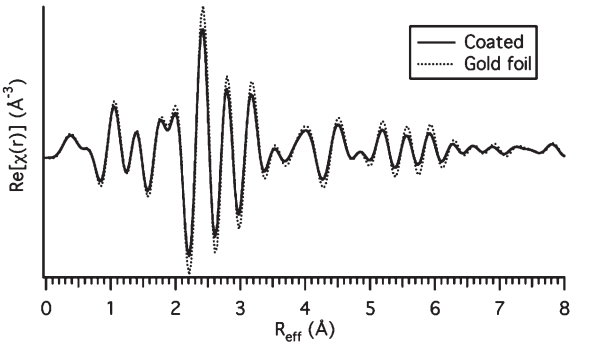

Figure 4. Real part of the Fourier transform of the EXAFS gold spectrum of the coated sample and the gold foil.

(Figure 3). For each edge, the Fourier transform of the data over a range of 4.0−10.0 Å^{-1} was taken, using Hanning windows with sills of size 1.0 Å^{-1}.

Figure 4 shows the Fourier transform for the gold edge, along with a Fourier transform of a gold foil, processed the same way. Although there is a slight suppression of amplitude of the sample Fourier transform relative to the foil, this suppression is not strongly dependent on k or R_{eff}, mimicking a difference in the EXAFS amplitude reduction factor. This suggests it is attributable to inhomogeneities introduced during sample preparation rather than to disorder or to reductions in coordination number due to nanoscale morphology.[14] Most of the gold in the sample is therefore present in the form of bulklike crystalline regions at least 10 nanometers across (see section 3.4).

(12) Rehr, J. J.; Albers, R. C. *Rev. Mod. Phys.* **2000**, *72*, 621–654.
(13) Newville, M.; Livins, P.; Yacoby, Y.; Rehr, J. J.; Stern, E. A. *Phys. Rev. B* **1993**, *47*, 14126–14131.
(14) Calvin, S.; Miller, M. M.; Goswami, R.; Cheng, S. F.; Mulvaney, S. P.; Whitman, L. J.; Harris, V. G. *J. Appl. Phys.* **2003**, *94*, 778–783.

For the iron edge, theoretical standards were then calculated using Feff6L.[15] As a starting structure for the cementite phase, the 300 K structure from ref 16 was used,[16] modified for a 1.5 nm diameter core following the method in ref 17. This structure has two distinct iron environments; a total of 87 direct-scattering and 107 associated multiple-scattering paths were incorporated in this standard. In contrast, a single direct-scattering path was used for the oxide phase, as the fraction of oxide present based on Mössbauer and XANES data suggests that the oxide is limited to a monolayer or less.

These standards were fit to the Fourier transforms of the data over the range of 1.2 to 4.0 Å, yielding 10.7 independent points for each sample according to the Nyquist criterion. Fits to both the coated and uncoated samples were corefined, so that S_o^2 (the EXAFS amplitude reduction factor) and E_o (the energy origin for the photoelectron) for the cementite phase could be constrained to be the same for both samples. (The E_o for the oxide phase was constrained to be 1.0 eV greater than for the cementite phase.) Five additional parameters were allowed to vary separately for each sample: a scale factor for the cementite, the nearest-neighbor distance for the oxide phase, and three factors parametrizing the mean-square radial displacement (MSRD). (The three parameters for MSRD's assigned one MSRD for the first shell of Fe−Fe paths, another for the first shell of Fe−C or Fe−O paths, and one for more distant paths. It may be objected that there is no a priori reason that the first-shell MSRD for Fe−C paths in cementite should be the same as the MSRD for the Fe−O path in the oxide layer. Although this is true, the Fe−C paths have very little effect on the fit, both because carbon atoms do not scatter strongly and because the relatively low symmetry of the cementite structure places carbon atoms at many different but similar distances, so that their contribution tends to cancel out. To confirm this, we attempted fits with the MSRD for the first-shell Fe−C paths constrained to the first-shell Fe−Fe paths; these fits were substantially the same as the ones presented here.) Thus, there were $10.7 \times 2 - (2 + 5 \times 2) = 9.4$ degrees of freedom in the fit.

For purposes of the EXAFS fits, the fraction of cementite in the coated sample was constrained to 45% in the coated sample and 70% in the uncoated sample for consistency with XANES. In addition, the average coordination for the oxide phase was assumed to be 3, as the proportion of oxide implies a monolayer or less on the surface of the particles. Both of these assumptions are a possible source of systematic error in the fits. To determine the extent of this error, we also attempted fits with the coated sample at 55% cementite and the uncoated sample at 80% (errors in the XANES determination are likely to be in the same direction), and in a separate fit, with the coordination number for oxygen at 2 rather than 3.

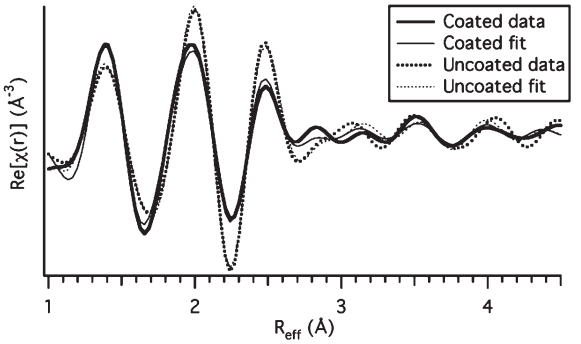

Figure 5. Fits to real part of Fourier transform of iron EXAFS.

Table 1. Results of Fits to EXAFS Spectra (Uncertainties in the Last Digit Shown Are Given in Parentheses)

	coated	uncoated
S_o^2	0.76(20)	
E_o	7115(3) eV	
cementite scale factor	0.983(9)	0.985(8) Å
iron−oxygen distance	1.89(3) Å	1.87(5) Å
first-shell Fe−Fe MSRD	0.002(11) Å^3	0.001(8) Å^3
first-shell Fe−O MSRD	0.001(14) Å^3	0.001(10)Å^3
MSRD for more distant paths	0.012(9)Å^3	0.013(6)Å^3
R factor	0.018	0.012

The results of the primary fits are given in Figure 5 and Table 1. Uncertainties given in the table include estimates drawn from the alternate fits of the possible contribution of systematic error from the XANES-based constraint on cementite fraction and the assumption of an average oxygen coordination number of 3. The *R* factor, given in the bottom row of the table, is widely used in the EXAFS community as a measure of closeness of fit. An *R* factor of zero would indicate a perfect match between fit and data; values below 0.02 are often considered to be "good" fits in the sense of matching the data well. Fits to other iron structures, including BCC, FCC, and icosahedral, were also attempted. None of these possibilities resulted in fits that were as satisfactory as the ones employing the cementite core.

3.3. Mössbauer Characterization. Mössbauer analysis carried out at 4 K revealed a resolved hyperfine fields (HPF) structure indicating the existence of two sites for the zerovalent Fe in the core: One site with a HPF field of 220 ± 3 kOe (39% relative absorption among the carbides), and the other at 252 ± 3 kOe (61% relative absorption). The presence of the 252 kOe splitting is indicative of iron in the cementite structure, Fe_3C.[18] This can be considered as the value observed for the Fe in the real core of cementite. In these nanoparticle metallic iron systems, it is to be expected when moving to the surface to observe an increase in the magnetic moment, but a decrease in the hyperfine field. To date, there have been no reported calculations for cementite (a metallic iron charged with some carbon atoms), to separate the HPF of

(15) Rehr, J. J.; Albers, R. C.; Zabinsky, S. I. *Phys. Rev. Lett.* **1992**, *69*, 3397–3400.
(16) Wood, I. G.; Vocadlo, L.; Knight, K. S.; Dobson, D. P.; Marshall, W. G.; Price, G. D.; Brodholt, J. *J. Appl. Crystallogr.* **2004**, *37*, 82–90.
(17) Calvin, S.; Luo, S. X.; Caragianis-Broadbridge, C.; McGuinness, J. K.; Anderson, E.; Lehman, A.; Wee, K. H.; Morrison, S. A.; Kurihara, L. K. *Appl. Phys. Lett.* **2005**, *87*, 183108.
(18) Marco, J. F. *Hyperfine Interact.* **2002**, *139/140*, 535.

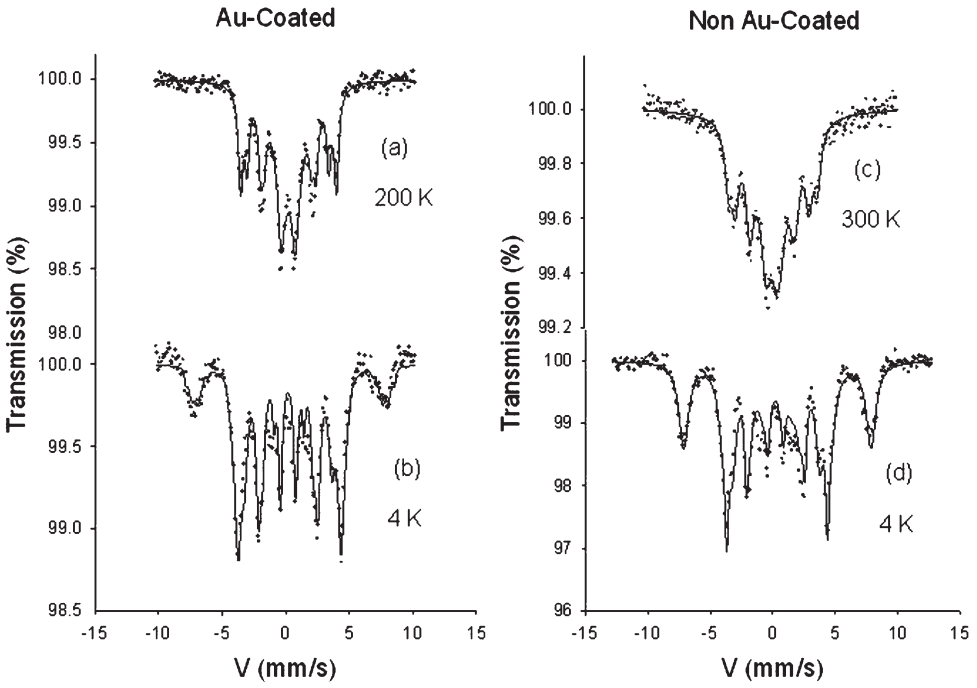

Figure 6. Mössbauer spectra of Au-coated and non Au-coated samples.

the core from surface atoms. Freeman and co-workers[19] have demonstrated that the HPF for iron has two components, a core HPF contribution, H_c, proportional to the magnetic moment, and a valence contribution, H_v, which is very sensitive to changes in the environment of the surface. This 220 kOe HPF observed is the sum of H_c and H_v, which are the irons closer the surface of the spherical cementite nanoparticle. In the bulk, the H_C and H_V are very similar unless the surface irons are altered through some surface treatment. In these spherical cementite nanoparticles, the H_V is very different, resulting in an augmented H_V to give the HPF total of 220 kOe. An important conclusion is that the iron oxide layer present is superparamagnetic in nature, and is almost completely in slow relaxation at 4 K. The form of the oxide shell was not similar to magnetite or to a typical iron oxide, thus corroborating the XANES and EXAFS structural results. Instead Mössbauer suggests that the iron oxide is a 3^+ valence, closely resembling an antiferromagnetic Fe−O structure.

Analysis was also performed on the uncoated sample. Evident differences in the Mössbauer spectra, primarily in the oxide layer, were observed between the Au-coated and non Au-coated samples. As for the uncoated case, the analysis of the spectra for both samples at 4 K is based on three components: two with hyperfine fields which correspond to cementite (HPF = 252 ± 3 kOe, the normal value for cementite at 4K,[18] and HPF = 220 ± 3 kOe for irons near from surface), and the third one corresponding to an oxide in slow relaxation (at room temperature it is in a superparamagnetic state). The nominal relative proportion of the oxide layer increases from 25% in the Au-coated sample to 43% in the uncoated case (corresponding spectra in Figure 6). In Figure 6a at 200 K the superparamagnetic (SPM) behavior of the oxide is clearly seen in a central doublet, which we assign to paramagnetic Fe^{3+}, whereas in Figure 6b at 4 K the doublet is transformed into a fully split magnetic spectrum (six lines, where only the two outer lines are clearly visible, whereas the remaining four are embedded in the central part of the spectrum) broadened because of a hyperfine field distribution (HPF ~432−512 kG), indicating a poor crystallization or a one-layer oxide.

It is important to note that although Mössbauer and XANES give different results for the oxide fractions in the two samples, Mössbauer does show evidence of broadening in some cases. This local disorder modifies the fractions found by the Mössbauer technique, but does not affect the XANES analysis. In panels c and d in Figure 6, the non Au-coated sample, a part from the carbide contributions described above, features at room temperature the characteristic doublet of the superparamagnetic Fe^{3+} contribution of an oxide, which at 4 K becomes a magnetic spectrum, more intense and well-defined oxide pattern (the two external lines clearly indicate this), compared with the Au-coated sample. It is interesting to point out that in principle we are observing a very original oxide, in the form of a spherical shell covering a ferromagnetic cementite nanoparticle.

3.4. Gold Shell Analysis. Mechanistically, the oxide layer formation occurs through Au^{3+} interacting with the Fe^0 and TOPO, resulting in the oxidation of the surface Fe with the TOPO being reduced to the phosphine, thus leaving a completely oxidized outer layer of iron with some Au coating the surface. The Au layer presence on the particles was shown by STEM-EDS (supplemental). This is also further corroborated by a

(19) Ruquian Wu; Freeman, A. J. *Phys. Rev. B* **1993**, *47*(7), 3904. Link, S.; El-Sayed, M. A. *J. Phys. Chem. B* **1999**, *103*, 4212–4217.

blue shift in the plasmon absorption maximum from 550 nm for pure Au nanoparticles (synthesized by PEG reduction as detailed before without iron seed addition) to 525 nm for the mixed solution of Au and Au coated cementite nanoparticles. The blue shift is indicative of an overall size reduction in the particles with Au surfaces, which would be the case for a mixture of both the 2−5 nm Au coated particles and the larger Au nanoparticles formed during the synthesis.[19] It has been presented in the literature that Au monolayers and thiol capped Au show ferromagnetism.[20,21] Thus, prior to magnetic analysis, it was necessary to determine if Au was present in a phase that might also contribute to the overall magnetization.

Powder X-ray diffraction revealed only sharp Au peaks, which by Scherrer analysis showed a crystallite size of 19 nm. Au EXAFS spectra were indistinguishable from bulk gold, confirming a mean crystallite size greater than 10 nm (also confirmed by TEM). This "large"-sized Au present in the sample can be treated as a mass dilution in the magnetic characterization. The Au present on the surface of the Fe_3C/FeOx/Au particles, however, could provide a contribution to the magnetization. From the Mössbauer analysis, the iron oxide formed on the surface acts as an antiferromagnetic layer. Because the metallic core is ferromagnetic, the FeOx-Au in the shell would take on an alignment with the core similar to a canted antiferromagnet, contributing a small amount to the overall magnetization. The presence of spin−orbit coupling between Fe and Au results in a slightly larger contribution to the overall magnetism than would be expected from a monolayer of typical FeOx alone. Because the amount of Au in the coating is undetermined, it is necessary to investigate the magnetic characteristics in terms of bohr magneton per atom of Fe. Elemental analysis by inductively coupled plasma-optical emission spectroscopy was used to directly determine the amount of Fe present in the sample used for magnetic analysis via super conducting quantum interference device magnetometry.

3.5. Further Magnetic Characterization. In the magnetic characterization of the Fe_3C/FeOx/Au particles, a zero-field-cooled/field-cooled plot revealed a blocking temperature of 170 K at 1000 Oe. This is much higher than expected and seen for Fe nanospheres of similar size.[9] To analyze the magnetic saturation, some assumptions had to be made first based on the structural information obtained from the XANES, EXAFS, and Mössbauer analysis. First, from the linear combination fits on the XANES edge, we used 45% for the zerovalent Fe and 55% for the oxide. Since Mössbauer indicated all Fe^{3+} for the oxide we assumed 3 mols of oxygen for every 2 mols of iron in the oxide. With this and the 3:1 mol ratio of iron to carbon in cementite, the mass was corrected utilizing these factors along with ICP-OES determined iron mass in the sample. A hysteresis loop at 10 K (Figure 7) showed a saturation magnetization of 110 emu/g and a coercivity of 1000 Oe. The M_R/M_S of 0.46 and coercivity of 1000 Oe is easily explained by the Stoner−Wohlfarth prediction for noninteracting single domain particles, which would be expected to have a M_R/M_S of 0.5.[22] The value of saturation magnetization, however, should be compared to 130 emu/g for bulk cementite, since the Fe_3C core has the largest diameter and thus better magnetic exchange than the oxide shell. This is impressively high especially for such a small nanomaterial utilizing the assumption of the highest oxygen content possible for an oxide. This gives possible implications of two modes for enhancement of the core magnetization. First, because the core is ferromagnetic and the shell shows antiferromagnetic arrangement from Mössbauer, there must be some inherent ordering of the shell that yields a net contribution to the moment. This could be possible with the shell taking on a particular direction of opposing alignment, thereby acting more as a canted antiferromagnet. Also, with the inclusion of Au in this shell, there is the possibility of spin−orbit coupling to further enhance this contribution and the overall magnetic moment.

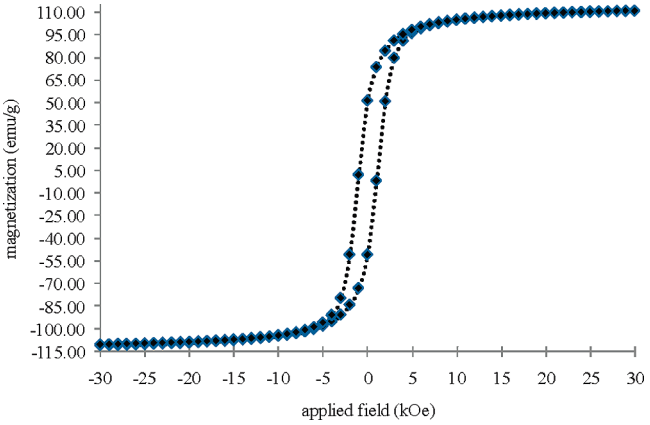

Figure 7. Plot of magnetization versus applied field for Fe_3C/FeOx/Au nanoparticles.

4. Conclusions

The picture that emerges from the use of Mössbauer and XAFS is clearly that of a core−shell nanoparticle, with a stable cementite core presenting very original HPF values corresponding to the very core irons and near surface irons, and a thin oxide shell. The structure and crystallinity of the shell depends crucially on whether the particle is coated with gold. The presence of gold provokes a faster kinetics of oxide formation thereby reducing the crystallinity of the shell. This reduced crystallinity might lead to an important subestimation of the proportion of the surface oxide using Mössbauer,

(20) Crespo, P.; Litran, R.; Rojas, T. C.; Multigner, M.; de la Fuente, J. M.; Sanchez-Lopez, J. C.; Garcia, M. A.; Hernando, A.; Penades, S.; Fernandez, A. *Phys. Rev. Lett.* **2004**, *93*, 177206.
(21) Yamamoto, Y.; Miura, T.; Suzuki, M.; Kawamura, N.; Miyagawa, H.; Nakamura, T.; Kobayashi, K.; Teranishi, T.; Hori, H. *Phys. Rev. Lett.* **2004**, *93*, 116801-1–116801-4.
(22) Stoner, E. C.; Wohlfarth, E. P. *Philos. Trans. R. Soc. London, Ser. A* **1948**, *240*, 599.

whereas the agreement between the two techniques for the more crystalline uncoated samples is closer. Passivation against oxidation has been confirmed by comparing the structure and relative amounts of Fe versus Fe−O in samples that were not exposed prior to analysis to other samples that were exposed for more than 4 months; all results remained consistent. Iron core−shell particles that have a BCC core are prone to oxidation over time because of a lattice mismatch between the BCC and FCC structure of the oxigens in the oxide. Since the cementite structure is similar to FCC, the lattice match to the oxide shell is close enough to allow for passivation. A further factor that stabilizes the Fe_3C/FeOx/Au nanoparticles is simply that cementite itself is not as prone to oxidation as typical BCC iron and thus when synthesized in this magnetic state, it can be more stable for multiple magnetic nanoparticle applications.

Acknowledgment. F.G.J. acknowledges some remarks from Pierre Bonville (Saclay, France) concerning cementite and the collaboration of Maria Bello on the fits of the Mossbauer spectra.

Supporting Information Available: Scanning transmission electron microscopy (STEM) image of Fe_3C/FeOx/Au nanoparticles combined with energy-dispersive spectroscopy (EDS) lines and zero-field-cooled/field-cooled plot of Fe_3C/FeOx/Au nanoparticles (PDF). This material is available free of charge via the Internet at http://pubs.acs.org."